Arch. Metall. Mater. **63** (2018), 1, 45-54

DOI: 10.24425/118907

P. MYŚLIWIEC*, R.E. ŚLIWA*#

FRICTION STIR WELDING OF THIN SHEETS OF MAGNESIUM ALLOY AZ31B

Friction stir welding developed in early 90's is a refreshing approach to the joining of different kinds of metals. FSW has become increasingly popular and provides excellent alternative to conventional welding or riveting sheets of various metals. The paper present the results of research work on linear FSW joining magnesium alloys AZ31B of 0.5 mm in thickness. The study was conducted on properly adapted numerical controlled 3 axis milling machine using a own made tools and fastening device. The tool dimensions have been estimated in accordance with the algorithm shown in the literature [2]. All joints were made of end-to end (butt) configuration under different process parameters. The effect of selected technological parameters on the quality of the joint was analyzed. Produced butt joint have been subjected to a static tensile testing to identify mechanical features of the materials of joints compared to parent materials. Measurements of micro hardness HV in the plastically formed stir zone of joint and in the parent material have been carried out. Axial and radial welding forces in the joining region were recorded during the tests and their dependency from the welding parameters was studied . Based on results of strength tests the efficiency of joints for sheets of 0.5 mm in thicknesses oscillated up to 90% compared to the parent material. It has been found that for given parameters the correct, free of defects joints were obtained. The results suggests that FSW can be potentially applied to magnesium alloys.

Keywords: FSW welding, magnesium alloys AZ31B, thin sheet, joining of metal sheets

1. Introduction

In recent years, the transportation industry especially the automotive and aviation sectors strongly committed to reducing the mass of the construction. Where weight reduction is one of the major critical factor for reducing fuel consumption and the emission of CO_2 into the environment. The process of weight reducing of a vehicle / aircraft mainly is carried out by replacing steel components by lightweight materials such as aluminum and magnesium alloys or composite materials. It has been observed increasingly, utilization of composite materials in modern automotive or aircraft structure constructions. Mutlimaterial structures are now becoming very common, and through the use of modern construction materials it is possible to decrease the mass construction up to 30%. Unfortunately, using a variety of materials causes technological difficulties in joining them, either the same kind of materials and combinations of different types of structural materials such as steel – aluminium or aluminum - plastic. The most frequently used techniques for joining materials are conventional welding, resistance welding RSW, gluing, riveting, detachable connection, laser welding, electron beam welding. However, the above-mentioned techniques not always make full use the potential of the joining material, are lessprofitable or cannot be used. Conventional welding methods have some limitations for joining magnesium alloys of their large energy requirement and strong cracking susceptibility [5]. FSW method seems to provide higher potential for joining magnesium alloys, because during the Friction Stir Welding process joining of the base material takes place without melting them. No melting takes place during the process, thus maintaining reality low temperatures and producing good quality joints with significantly low residual stresses [6]. Magnesium alloys can be joined using a wide variety of process, but conventional process have exhibited several disadvantages such as large Heat Affected Zone, porosity, evaporative loss of the alloying elements, and high residual stresses [6,24-26].

In recent years we have seen growing interest of the FSW process. This method was developed at the University of Cambridge in the early 90s, [1] in particular, for joining materials such as precipitation-hardening aluminum alloys series 2xxx and 7xxx classified as material not weldable with conventional methods, but recently it has been implemented to weld other materials. FSW offers numerous advantages and potential for cost reductions in each of these cases. FSW process is friendly to the environment. The process lacks of toxic fumes, shielding gases and doesn't require post welding processing [8]. Evidence of this several times lower energy balance compared to arc welding or resistance welding RSW. In addition, the FSW process does not require the use of shielding gases, special surface preparation of joined materials, does not generate noise. Application of FSW

* RZESZOW UNIVERSITY OF TECHNOLOGY, 12 POWSTAŃCÓW WARSZAWY AV., 35-959 RZESZÓW, POLAND

Corresponding author: r.sliwa@prz.edu.pl

also contributes to a smaller deformation of the joined elements, in contrast to conventional welding. Using this method it is possible to perform joints using other construction materials such as magnesium alloys, mild steel, nickel alloys, titanium and combinations of materials such as aluminum-magnesium alloys, aluminum-copper-aluminum or even steel. Direct comparison of FSW welding technology to a conventional welding, shows a better mechanical properties, greater resistance to bending or higher fatigue. All these features ensure that the FSW process is becoming used more widely in many industries such as. automotive, shipbuilding and aerospace [3,4].

The FSW process takes place in solid phase at temperature below the melting point of the material, and as result does not experience problems related to resolidification , such as the formation of second phase, porosity, embrittlement and cracking. In additional the lower temperature of the process enables joining with lower distortion and lower residual stresses [7].

The principle of operation of the process is relatively simple. Non consumable rotating tool is placed inside the welding line (Fig. 1). The heat generated from shoulder of the tool causes the material to become soft and enables it to flow and be stirred. Simultaneously, the rotating shoulder is located on the surface of the plates which generates frictional heat and avoids the material flash leakage out of the seam, providing a smooth surface [8]. Modification of microstructure in the center zone of FSW joint largely caused by the secondary dynamic recrystallization of the material and the formation of even an order of magnitude smaller axial equal grain. This phenomenon may cause slightly decrease the mechanical properties of the joint. It is important to choose the appropriate technological and geometrical welding parameters. Although, the optimization of the welding parameters such as tool rotation speed; tool feed (welding speed) is critical to obtain high quality welds, the optimization of the tool geometry and tool material are also very important [9]. This allows for producing defect-free joints characterized by good mechanical properties. However, the material flow behavior is predominantly influenced by the FSW tool profile, tool dimension and process parameters [10].

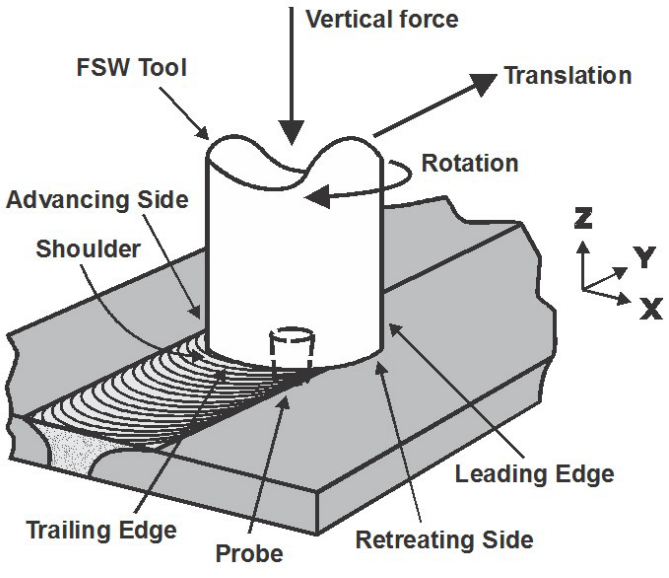

Fig. 1. Scheme of linear Friction Stir Welding process

Another important aspect under investigation are the forces generated by the tool action during realization the FSW process and the effect of the process parameters on them. The vertical and horizontal forces are fundamental to fully understand the welding process, furthermore, their knowledge provides data for the process parameters optimization [11]. In practice the value of the measured force can be also used in order to develop an adaptive control system; to this end, the process parameters are adopted in order to keep forces measured during FSW at the values providing the optimal combination of joint properties [11, 12]. It is known that the rotational speed of the FSW tool and welding speed of the tool have a strong effect on heat generation, heat dissipation and cooling rate, therefore the joint formation, microstructure of the weld and forces are affected by the rotational speed and tool feed value. Increasing the rotational speed of the FSW tool leads to higher temperature and cause more intensive mixing of the joining material. On the other hand, increasing the tool feed rate produces a decrease in specific thermal contribution conferred to the joint so that less time is given to the heat to flow into the joint. For these reasons the welding technological parameters must be carefully chosen in order to ensure a successful and efficient FSW process [13,14,18].

The properly made FSW joints has the following characteristics zone shown on Fig. 2. As a result of process mechanism and heat generation it was found that the FSW joints are composed of two main zones. First zone located in center of cross-section of the weld usually named Nugget or SZ (Stirred Zone), it is fully recrystallized region. Another zone is HAZ (Heat Affected Zone) and the next to is TMAZ (Thermo-Mechanically Affected Zone). Meanwhile in the HAZ the material experienced thermal conditions that modified its microstructure and mechanical properties without any plastic deformation, in the TMAZ, the material was hardly plastically deformed at high temperatures under the action of the FSW tool [16,17]. Each zones has a different thermo-mechanically history [6]. In addition depending on the tool rotating rate and traverse speed. The SZ can contain a ring pattern or other microstructural variation [6]. The deformation under the shoulder region is likely to influence the final texture significantly. This point is fundamental because texture influences a variety of properties including strength ductility, formability, and corrosion resistance [6]. Properly made FSW joint has a very good mechanical properties in relation to the parent material, UTS may reach up to over 90% in relation to the

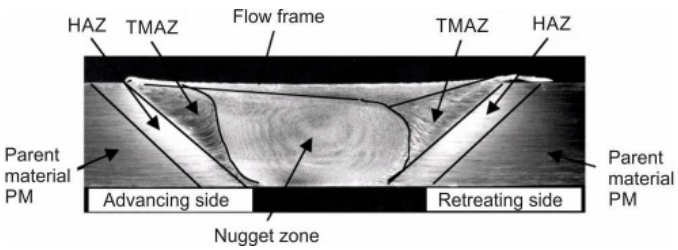

Fig. 2. Cross-section of the process zone of material. Overview of micrographs from the BM, HAZ, TMAZ and SZ of the sample

parent material. For instance the strength of the joint fabricated thought the conventional fusion welding methods can only reach up to 50-70% for the parent material.

The paper presents the characteristics of the dynamic nature of the process FSW-based on plasticizing effect of joining materials and their mixing in the welding zone with particular emphasis on the specifics of joining very thin sheets of metallic materials. Numerous studies on the linear FSW process for joining materials of different thickness have been presented, but very little work relates to the welding of very thin sheet metal alloys used in aviation, hence the need for further research. The aim of present research was to prove the feasibility of FSW very thin sheets of magnesium alloy AZ31B. The effect of the welding technological parameters on the microstructure and mechanical properties of AZ31B alloy was also studied.

2. Experimental procedure

The initial material used in this work is a cold-rolled commercial AZ31B magnesium alloy (Mg-3%Al-1%Zn) plate with the 0.5 mm in thickness. Magnesium has high affinity for oxygen, and thus, the surfaces of magnesium alloys are usually covered with oxide films. Magnesium oxide is porous and can absorb some moisture, leading to the formation of magnesium hydroxides [20]. In this investigation, the joining region are carefully cleaned prior to welding, but the oxides cannot be removed thoroughly. After polished by abrasive paper and cleaning with acetone, several weld plates were subjected to FSW along the rolling direction. The blank sheet dimentions were 180×100 mm. A backing plate witch two holders constituted the fixture to firmly hold the workpiece. Fixing device with workpiece was installed on the plate of piezoelectric Kistler dynamometer shown on Fig. 3a. The FSW experiments were carried out on a special adopted CNC milling machine (Fig. 3b) using the welding tool shown on Fig. 4. Non consumable cylindrical tool made from tungsten carbide with geometrical features reported in Table 1.

TABLE 1

Inputs used for the experimental set-up of FSW

Tool material	**Tungsten carbide**
Shoulder diameter D	10
Pin diameter d	3
Pin height	0,45
Pin profile	cylindrical
Shoulder profile	Flat
D/d ratio of the tool	3
Dwell time	20 s

The tool has been made in the hard micro-milling process. The tool design greatly influences to the plastic flow of welding material, heat generation and the uniformity of the welded joint. Tool dimension was adjusted to the material sheet thickness according to algorithm [18] shown in literature. Generally we can assume that the ratio of shoulder diameter to pin diameters is around 3. Both the pin and the shoulder of the tool have smooth cylindrical shape. Tool worked without a tilt angle, perpendicular to the surface of the welded material.

The butt joint configuration was prepared to produce the joints. Welding has been done on the 180 mm long section. The welding condition were systematically adjusted until defect-free process zones were obtained. The welding conditions and tool parameters used for welding in this work are listed in Table 2. Shoulder plunge depth was chosen as 0.05 mm. FSW welding experiments were carried out with constant values of rotational speed and welding speed in the range from 2000 to 4000 RPM and tool feed from 80 to 120 mm/min. The dwell time was the same for all joints and was 20 s. Tool plunging in and out stages was realized with tool feed rate equal 5 mm/min. Visual

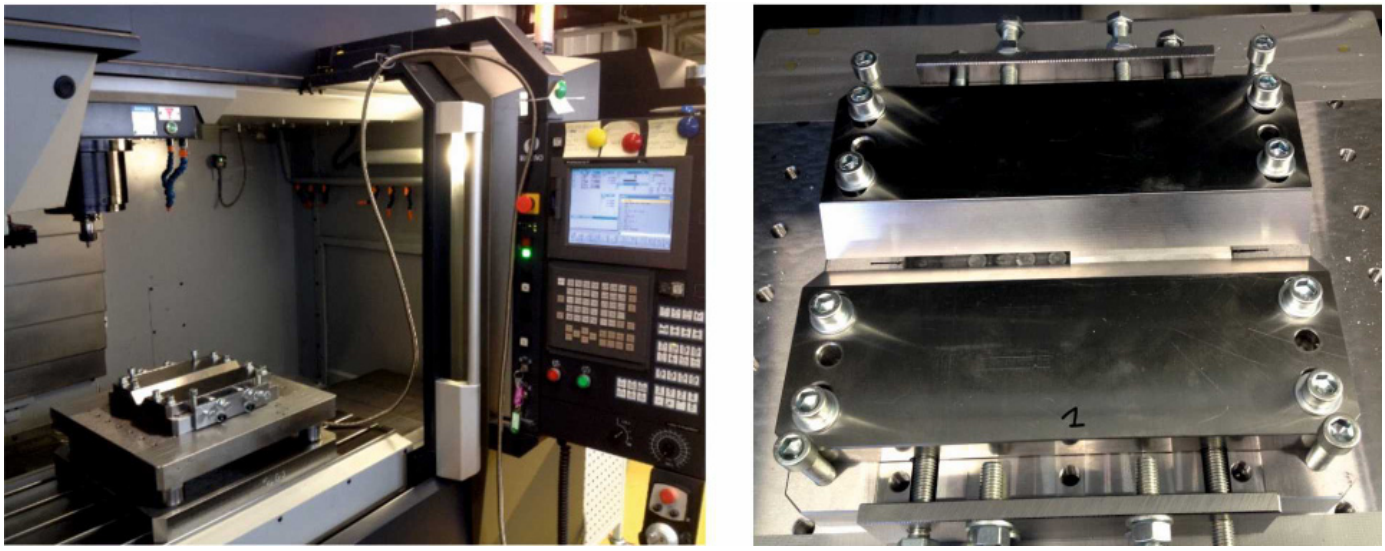

a) b)

Fig. 3. a) general view of 3-axis CNC machine adopted for FSW process, b) view of mounting device used in FSW process

TABLE 2

Linear FSW technological parameters, joints and parent material mechanical properties and experimental results of Mg alloys 0,5 mm in thickness

Material AZ31B Set:	Rotational speed [RPM]	Welding speed [mm/min]	Weld pitch	UTS [MPa]	YS $R_{0,2}$ [MPa]	Total elongation [%]	Joint effectiveness [%]
1.	2000	100	0,050	250	194	1,56	87
2.	3000		0,033	195	148	1,18	68
3.	3500		0,029	238	189	1,8	83
4.	4000		0,025	224	184	1,18	78
5.	2000	80	0,040	260	202	2,49	90
6.	2000	120	0,060	185	135	0,8	65
Parent material				286	207	8,4	

evaluation of FSW joints showed that they are done properly, have no visible defects, face and root surface was smooth and uniform (Fig. 5). No flash means more plastic material flows into the joint [19].

Fig. 4. The tool used in Friction Stir Welding process made from tungsten carbide

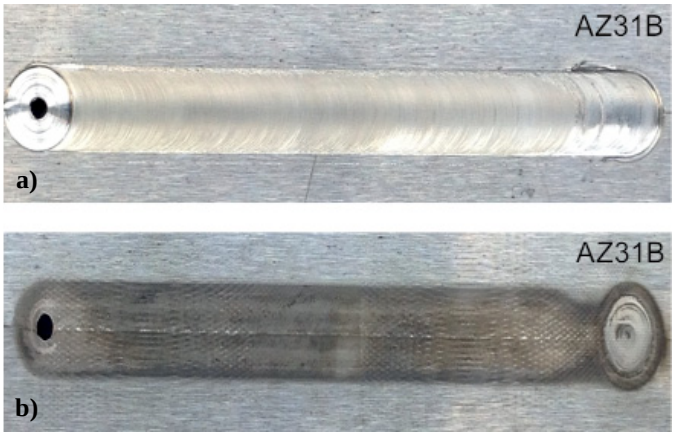

Fig. 5. Photographic view obtained FSW joint of the AZ31B magnesium alloys, a) face of joint, b) ridge of joint

2.1. Tensile testing of FSW joints

Obtained FSW joints were the basis to make specimens for tensile tests and metallographic examinations. The mechanical properties of the joints were measured during tensile testing, as well as micro hardness testing. Tensile specimens dimension was shown on Fig. 6. Dumbell specimen preparation was performed using wire EDM machining.

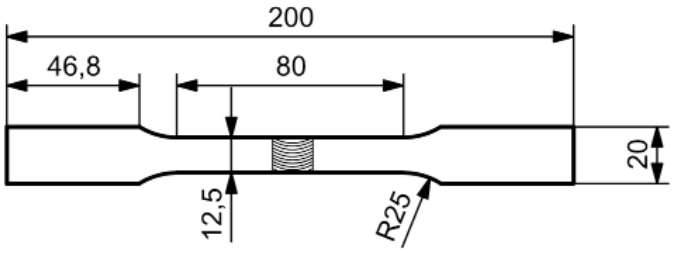

Fig. 6. Uniaxial tensile testing geometry (dimension are in mm)

Static tensile test was performed in accordance with PN-EN ISO 6892-1:2009. The tensile tests were carried out on an Zwick/Roell Z 100 universal testing machine shown on Fig. 7, at room temperature. An extensometer with a gauge length of 50 mm was used for strain data acquisition. The results, given by the nominal stress vs. nominal strain curves, were evaluated in terms of the ultimate tensile strength (UTS), yield strength (YS) and ultimate elongation (UE) in percentage. In the purpose of verifying the repeatability of the results each tested samples was repeated at least three times. From each joined metallic plate was cut three samples from the beginning, middle and end of a weld and then the measured values were averaged. Mechanical properties of FSW joints were grouped in the Table 2. Overall, it was observed that the base material exhibit higher mechanical properties than the FSW samples. The tensile properties of the joints are slightly affected by the rotational and welding speeds. The maximum force to elongation data for all coupons are plotted in figure 8.

It is seen that the after welding both the strength and elongation reduced. The Ultimate Tensile Strength (UTS) of BM (base material) was obtained to be 286 MPa. Joint efficiency of the FSW joints varied approximately from 65% to 90%. The

a) b)

Fig. 7. Universal testing machine, a) general view, b) view of fixture device

elongation were relatively low compared to the BM, ranging from 1.4% to 2.5%. During tensile testing, the failure of the sample was basically in the form of 45° shear fracture, which could be due to the significant change of texture with a high intensity of (0002) diffraction around the TMAZ during FSW, leading to a prone slip along the (0002) with an orientation of ~45° at a low critical resolved shear stress [20]. The failure of all FSW welds was observed to occur in between the SZ and TMAZ always on AS side for all welding condition. The UTS increased with increasing welding speed as well, which was observed by some researchers [20,21]. But the UTS could decrease beyond a certain welding speed due to the formation of the welding defects such as kissing bond. Due to the microscopic roughness or asperities or the oxides with some absorbed air, effective metallic bonding might not be well established in the solid state during FSW, leading to the formation of kissing bond defects at high welding speeds [22]. It should be noted that, the kissing bond was extremely difficult to detect with any non-destructive testing method due to its sub-millimeter size [22]. The overall reduction in the ductility after FSW would be due to the presence of a certain amount of kissing bond defects and/or lack-of-bonding defects occurred near the bottom surface for the FSW joints.

Several welding parameters have been tested in order to achieve the strongest welds using conventional tools. The best results was achieved when the rotational rate decreased from 4000 rpm to 2000 RPM We note that the best FSW joint has been obtained for the parameters set 10 from the table 1 for rotational

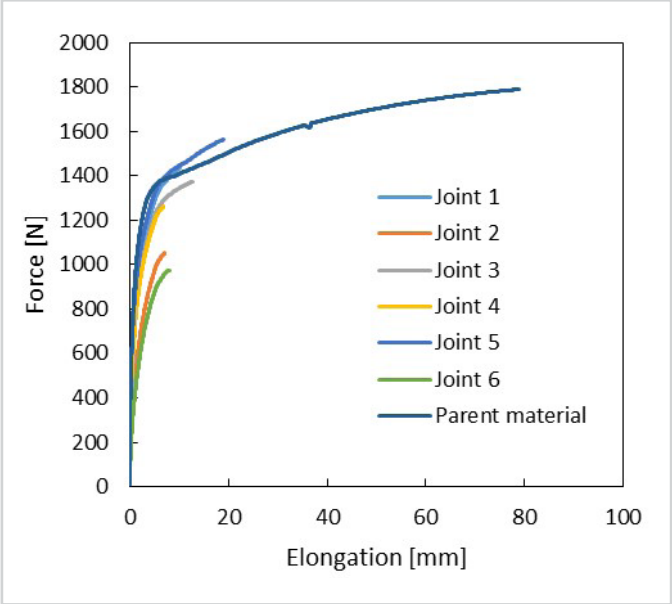

Fig. 8. Tensile tests results of FSW joint

speed 2000 RPM and welding speed 80 mm/min. The effectiveness of FSW joints was on the level 90% when compared to the base material. Further increase the welding speed caused gradual decline in UTS. The combined role of both the welding speed and rotational rate could be better represented by the weld pitch (v/ω). The strength of the FSW joint as a function of the weld pitch is plotted in Fig. 9.

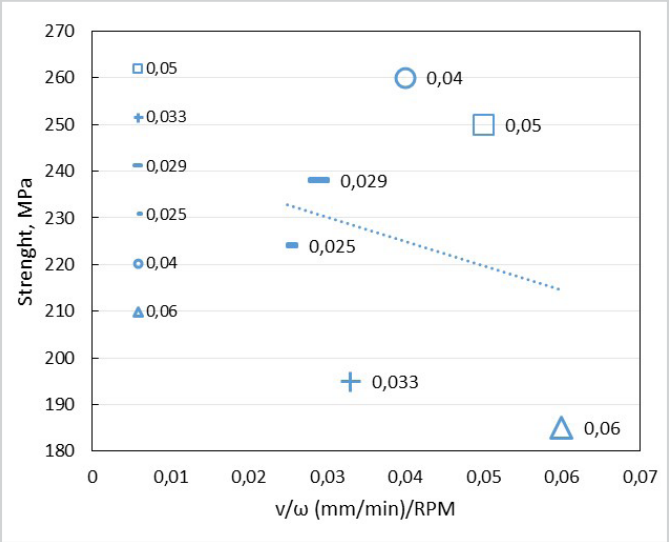

Fig. 9. A comparison of the UTS of the AZ31B weld joints as function of the weld pitch (the ratio of welding speed

2.2. Micro hardness tests of FSW joints

Material hardness was measured using a Vickers micro hardness tester NEXUS 4303 according to ASTM E382-16. Applied load equal 1N. Measurements were carried out on a cross-section of the plate in the area of the weld to approx. 20 mm. For each cross-section, an average of 40 indentations 0.5 mm apart, were made on the weld surface. This provided data from outside the stir zone on each edge of the weld, in order to determine how the welding parameters affected both the weld zone and HAZ. Hardness of the base material is between 70-75 HV. Fig. 10 and 11 shown 2 group of micro hardness profile of FSW joint. First group shown on Fig. 10 (welds 1-4) was made with constant welding speed. Increasing the rotational speed of the tool not significantly affected for micro hardness profile. Differences in hardness are very small. The common part of all charts is a slight decrease hardness in weld nugget zone. The base metal of AZ31 is work hardened so that the dislocation density of the base metal may be higher than the stir zone. The difference of the dislocation density may cause hardness decrease in the stir zone. Fig. 11. shown the micro hardness result for welds 5 and 6 performing with constant rotational speed (2000 RPM) and variables welding speed. The weld nugget shown a reduced hardness with respect to PM. For weld 6 the micro hardness value in stir zone was around 60 HV. It also had the worst mechanical properties of all welds.

2.3. Microstructure of FSW joints

For metallographic examination the samples were cross-sectioned perpendicular to the welding direction. The standard metallographic preparation method was used to prepare the specimens according to the E3 ASTM standards. Etching was performed using an acetic picral solution composed of 4.2 g picric acid, 10 ml acetic acid, 70 ml ethanol and 10 ml water.

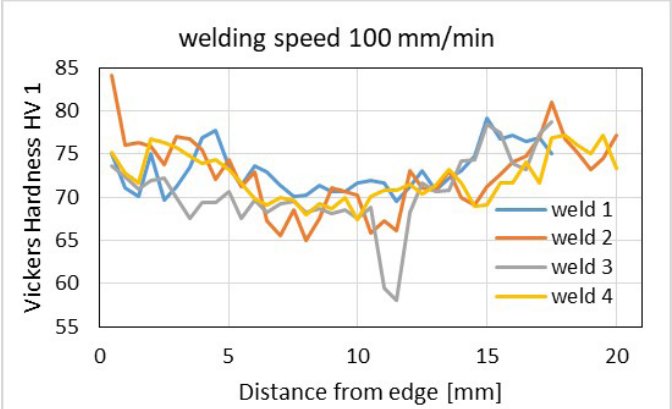

Fig. 10. 2D linear graph of the integration hardness measurements points along a line parallel to processing direction for welds 1 to 4

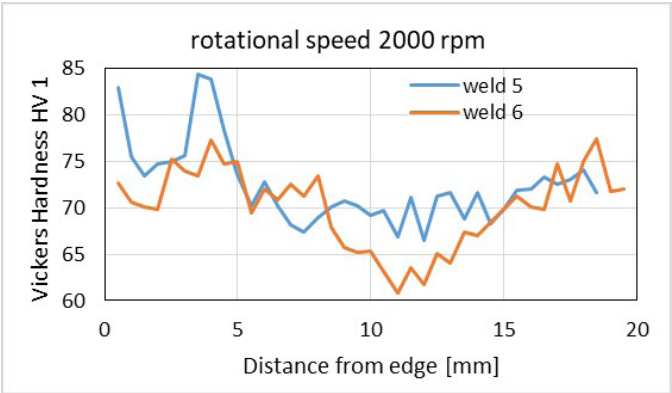

Fig. 11. 2D linear graph of the integration hardness measurements points along a line parallel to processing direction for welds 5 and 6

For microstructural and textural observation were taken using Nikon optical microscope and Hitachi SEM microscope.

Fig. 12 shows the microstructure of typical FSWed sample made at welding speed of 80 mm/min and rotational rate of 2000 RPM. On the cross section view is very hard to identify all of characterized zone of typical FSW welds. This is probably related to the welding of very thin sheets of metallic materials vice versa to the thicker sheets of metal. The location of the FSW joint characteristic areas can be determined by the dimensions of the tool. It is seen that the microstructure of the BM consisted of elongated and pancake-shaped grains grains with varying sizes (Fig. 12a). The heterogeneity of the grain structure of the BM was due to both deformation of the 0.5 mm in thickness sheet by rolling and incomplete dynamic recrystallization [21]. Equiaxed grains were observed in HAZ and TMAZ zone as shown in Fig. 12b. The presence of the equiaxed grains in the HAZ and TMAZ indicated that full recrystallization had taken placed during FSW process. The grains in the SZ were observed to be equiaxed as well and slightly larger mainly due to the dynamic recrystallization and grain growth as shown in Fig. 12c. Mg alloys might experience dynamic recrystallization more easily than Al alloys because the recrystallization temperature of Mg alloys was about 523 K, which was lower than that of the Al alloys in general [23]. During FSW the peak temperature experi-

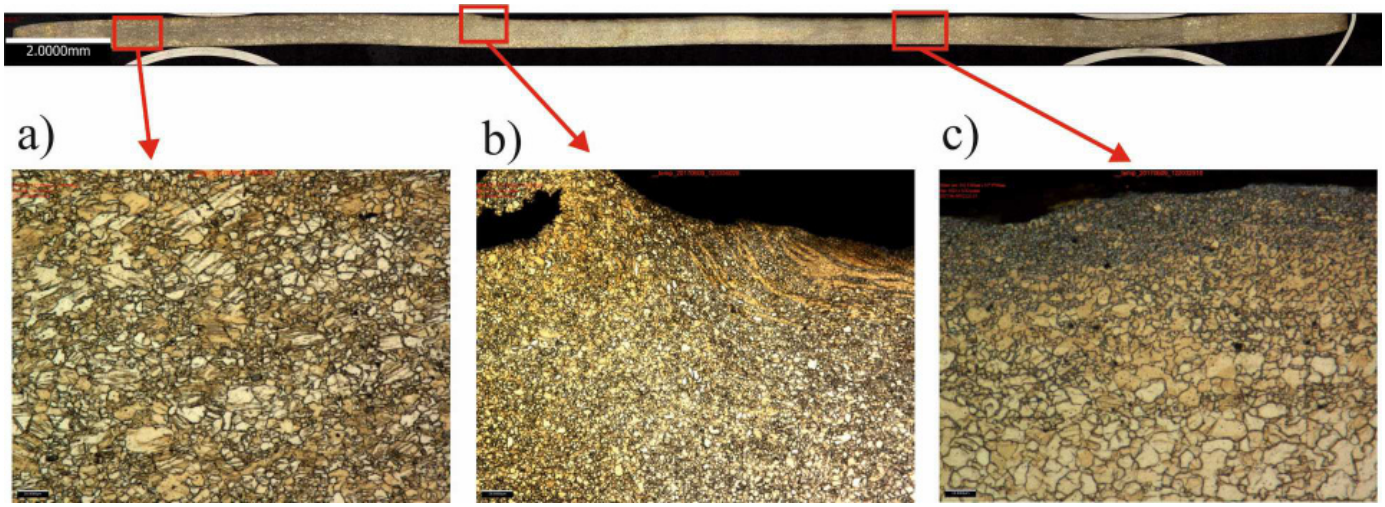

Fig. 12.Typical microstructures of a FSW joint made at different rotational speed and welding speed.
a) Microscopic structure of FSW welded AZ31B of 0,5 mm in thickness. View of base material BM
b) Microscopic structure of FSW welded AZ31B of 0,5 mm in thickness. View of HAZ and TMAZ zone from the retreating side
c) Microscopic structure of FSW welded AZ31B of 0,5 mm in thickness. View of stir zone SZ and TMAZ of advancing side

enced in these region (SZ, TMAZ) was higher than the dynamic recrystallization temperature for Mg alloys, so that the dynamic recrystallization in both SZ and TMAZ would be anticipated, as seen in Fig. 12c. On the upper layer of the FSW joint we can see the fine grain formed by the large plastic deformation coming from the rotating tool. Obtained FSW joint did not contain any visible defect in the form of cavities or lack-of-bonding defect.

2.4. Force measurements during FSW process

The vertical (Z axis) and horizontal (X,Y axis) forces occurring during linear FSW process was measured by high sensitive piezoelectric dynamometer developed by Kistler. It consist of four piezoelectric force sensor calibrated in range from 0 to 60 kN. Sensors were fitted between two rigid plates (400 mm long, 400 mm width and 50 mm in thickness each). The dynamometer is shown on Fig. 13. The all sensors were connected via adder to a single charge amplifier. The force data were acquired with a maximum sample rate per channel of 200 kS/s and 16-bit resolution. The actual sample rate used during the data recording was 1 kHz. The effect of the thermal drift of sensors on the values of forces measured during FSW process was preliminary investigated. The blank sheets are subjected to a significant heating during welding that can cause a dilatation of both quartz and housing with mounting screw and consequently a preloading reduction. Considering the size and thickness of the plate of the dynamometer the influence of heat from the FSW process for thermal drift is negligible.

Measurement of forces was conducted for all 6 samples. Figure 14 shows a typical vertical and horizontal forces versus time curve recorded during FSW of AZ31B Mg alloys of 0.5 mm in thickness. Presented graph (Fig. 14) belong to the FSW joint characterized by the best mechanical properties. Four different stages of FSW process can be recognized: (I) tool plunging, (II) tool dwelling, (III) welding, (IV) tool pulling out. During

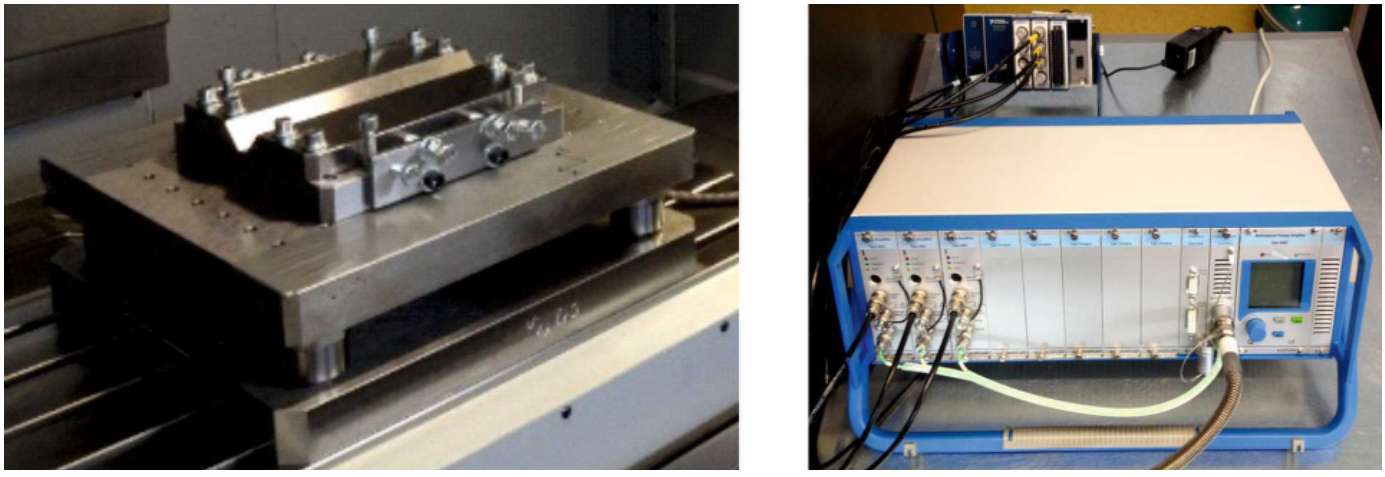

a) b)

Fig. 13. Force measurement device, a) piezoelectric dynamometer, b) charge amplifier

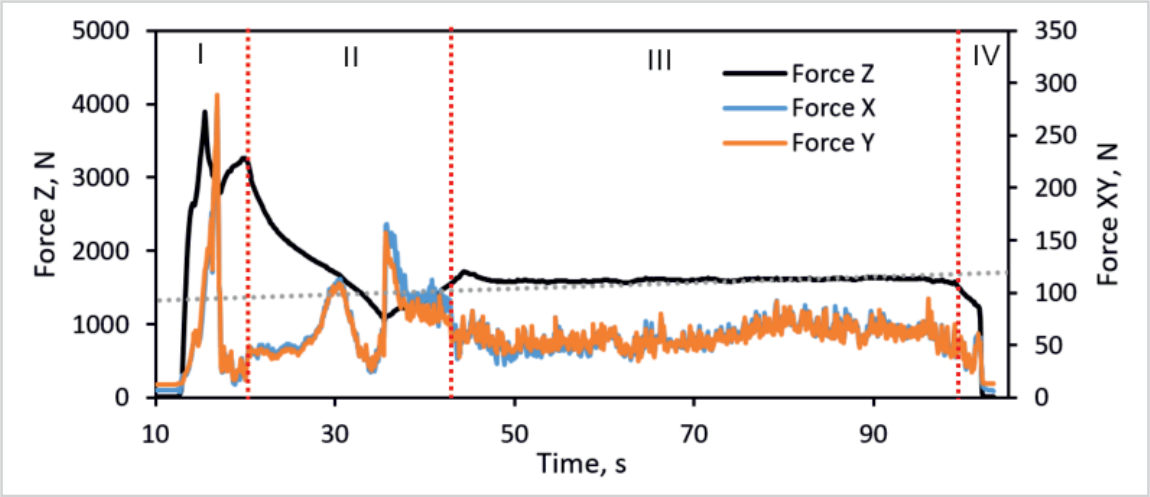

Fig. 14. Typical graph of the axial and translational forces versus time during FSW of AZ31B alloy sheet for ω = 2000 rpm, v = 80 mm/min witch marked stages

first stage tool plunges into the workpiece with an increase in the deformed volume [11]. Both vertical and horizontal forces rise quickly owning to the strength of the deforming material to the pin penetration that prevails on the softening due to the heat generated by the stirring action of the rotating pin. The local softening of the welded material promptly becomes the predominant effect and produces a decrease both vertical and horizontal forces [11]. Stage (II) is performed to assure an adequate heating of the blank material before welding. During the experiment dwelling time was constant and was 20s. Following with the literature increasing the dwell time does not affect on the quality of the FSW process [11]. For this reason, dwelling time not subject to modification. At the stage (III) the vertical and horizontal forces suddenly increases and as see on Fig. 14 the curve reaches almost steady state that is kept during the entire welding process.

The influence of rotational speed and welding speed especially on the vertical force was analyzed. Table 3 summarizes the welding parameters and the corresponding vertical and horizontal forces.

Average Z axis forces values during welding stage were in range from 1300 to 2200 N. Increasing rotational speed at constant welding speed of the tool causes decreasing the axial forces. When the rotational speed of the tool was constant increasing the welding speed caused also increasing the axial force. Determining the values of force during FSW process is also very helpful when selecting the right machine.

3. Conclusions

The results of this study demonstrated the microstructural and anisotropic modification induced by FSW in a thin sheet of magnesium alloys AZ31B in 0.5 mm in thickness. The results of this study reveal that FSW induces the generation of several distinct zones with different microstructural, anisotropic and mechanical properties. The following conclusions are drawn from this research.

1. Butt joints with smooth surface, without voids and flash can be obtained by cylindrical flat shoulder and pin tool made from tungsten carbide of the dimensions given in Table 1.
2. Tensile tests revealed a durability increase up to 90% compared to BM which is thought to be mainly attributed to the preferred basal orientation and the activation of the extension twins.
3. The SZ and TMAZ experienced full dynamic recrystallization and thus consisted predominantly of equiaxed grains. The grain size in SZ increased with increasing heat input.
4. During the FSW, the process must be carried out at the temperature preferably higher than the recrystallization temperature of the base material BM to be joined for the dynamic recrystallization to take place in the SZ.
5. With increasing tool rotational speed or decreasing welding speed supplied more heat energy and generated a higher

TABLE 3

FSW welding parameters with corresponding forces

Joint No.	Rotational speed [RPM]	Welding speed [mm/min]	Weld pitch	Max. force Z [N]	Max. force XY [N]	Average force during welding stage (Z axis) [N]
1	2000	100	0,050	3200	260	1600
2	3000	100	0,033	2750	200	1800
3	3500	100	0,029	2750	325	1300
4	4000	100	0,025	3500	275	1300
5	2000	80	0,040	3950	280	1600
6	2000	120	0,060	3950	325	2200

TABLE 4

View of FSW joints witch force measurements data

No.	Face of joint	Ridge of joint	Force plot
1.	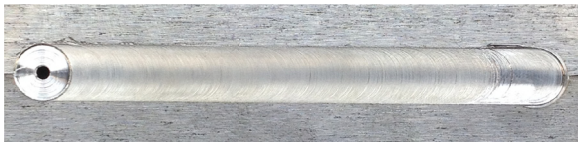		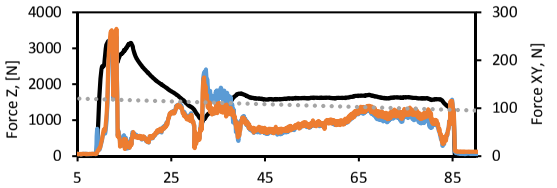
2.			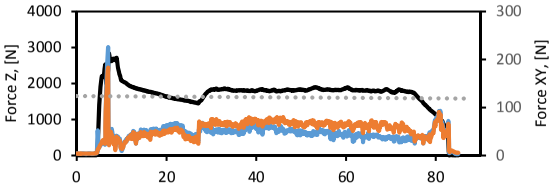
3.			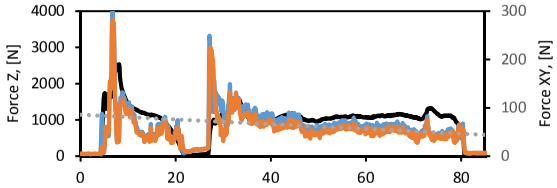
4.			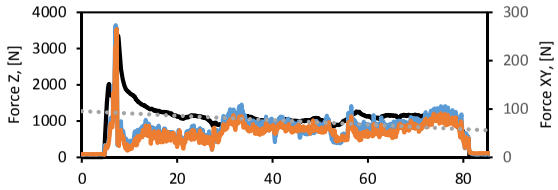
5.			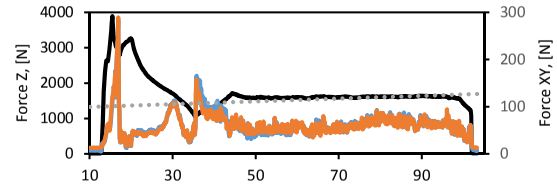
6.		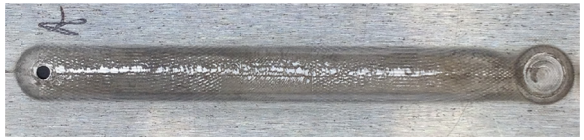	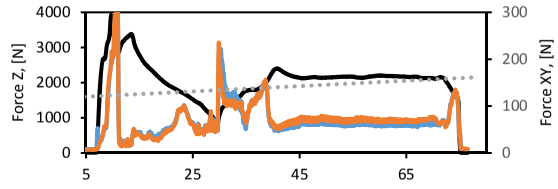

temperature in stir zone SZ. This led to a weaker or more random texture stemming from the occurrence of more complete dynamic recrystallization.

6. After the FSW of AZ31B alloy of 0.5 mm in thickness, the lowest hardness occurred at the center of SZ through the HAZ and TMAZ of the welded joints however, the differences are minor.
7. The welding speed and rotational speed had a strong effect on the UTS.
8. When choosing the technological parameters for the process, tool feed rate played an important role in compared to a tool rotation speed.
9. The plastic flow in the welded regions is also observed with uniform grain orientation.

Acknowledgements

Financial support of Structural Funds in the Operational Program Innovative Economy (IE OP) financed from the European Regional Development Funds Project "Modern material technologies in aerospace industry", Nr POIG.01.01.02-00-015/08-00 is gratefully acknowledged.

REFERENCES

[1] W.M. Thomas, E.D. Nicholas, J.C. Needham, M.G. Murch, P. Templesmith, C.J. Dawes, Friction Stir Butt Welding, International Patent Application PCT/GB92/02203, GB Patent Application 9125978.8. 6 Dec. 1991 and US Patent 5,460,317.

[2] Y.N. Zhang, X. Cao, S. Larose, P. Wanjara, Review of tools for friction stir welding and processing, Canadian Metallurgical Quarterly **51**, 3 (2012).

[3] P. Myśliwiec, R.E. Śliwa, Linear FSW Technology for Joining Thin Sheets of Aluminium and Magnesium Alloys, International Scientific Conference PRO-TECH-MA 2016, Bezmiechowa 2016.

[4] P. Lacki, Z. Kucharczyk, R.E. Śliwa, T. Gałaczyński, Effect of tool shape on temperature field in friction stir spot welding Archives of Metallurgy and Materials **58**, 597-601 (2013), DOI: 10.2478/amm-2013-0043.

[5] P. Sevcel, V. Jaiganesh, Effect of Tool Shoulder Diamater to Plate Thickness Ratio on Mechanical Properties and Nugget Zone Characteristics During FSW of Dissimilar Mg Alloys, The Indian Institute of Metals 41-46 (2015).

[6] A. Kouadri-Henni, L. Barrallier, Mechanical Properties, Macrostructure and Crystallographic Texture of Magnesium AZ91-D Alloy Welded by Friction Stir Welding (FSW), Metallurgical and Materials Transactions **45A**, 2014.

[7] B.T. Gibson, D.H. Lammlein, T.J. Prater, W.R. Longhurst, C.D. Cox, M.C. Ballun, K.J. Dharmaraj, G.E. Cook, A.M. Strauss, Friction stir welding: Process, automation, and control, Journal of Manufacturing Processes **16**, 56-73 (2014).

[8] S. Eslami, T. Ramos, P.J. Tavares, P.M.G.P. Moreira, Shoulder design developments for FSW lap joints of dissimilar polymers, Journal of Manufacturing Processes **20**, 15-23 (2015).

[9] A. Dobrane, G. Ayoub, B. Mansoor, R.F. Hamade, G. Kridil, R. Shabadi, A. Imed, Microstructural observations and tensile fracture behavior of FSW twin roll cast AZ31 Mg sheets, Material Science & Engineering A **649**, 190-200 (2016).

[10] G. Rambabu, D. Balaji Naik, C.H. Venkata Roa, K. Srinivasa Roa, G. Madhusudan Reddy, Optimization of friction stir welding parameters for improved corrosion resistance of AA2219 aluminum alloy joints, Defence Technology **11**, 330-337 (2015).

[11] A. Forcellese, M. Martarelli, M. Simoncini, Effect of process parameters on vertical forces and temperatures developed during friction stir welding of magnesium alloys, Int. J. Adv. Manuf. Technol. **85**, 595-604 (2016).

[12] P. Sevvel, V. Jaiganesh, Characterization of mechanical properties and microstructural analysis od friction stir welding AZ31B Mg alloy thought optimized process parameters, Procedia Engineering **97**, 741-751 (2014).

[13] X. He, F. Gu, A. Ball, A review of numerical analysis of friction stir welding, Prog Mater Sci **65**,1-66, 2014.

[14] A. Astarita, A. Squillace, L. Carrino, Experimental study of the forces acting on the tool in the friction stir welding of AA 2024 T3 sheets, J. Mater. Eng. Perform. **23** (10), 3754-3761 (2014).

[15] I. Galvao, C. Leitao, A. Loureiro, D. Rodrigues, Friction Stir Welding Very Thin Plates.

[16] R.S. Mishra, Z.Y. Ma, Friction stir welding and processing, Materials Science and Engineering R **50**, 1-78 (2005).

[17] TWI, Microstructure classification of friction stir welds, Avaible in: www.twi.co.uk/content/fswqual.html , 2010.

[18] Sheng L, Xingyin Z, Bin L, Yunpeng W, Effects of Workpiece Size on Temperature Distribution during FSW of AZ31 Magnesium Alloys, Materials Science Forum, 734-741, 2016.

[19] Z. Zhou, Y. Yue, S. Ji, Z. Li, L. Zhang, Effect of rotating speed on joint morphology and lap shear properties of stationary shoulder friction stir lap welded 6061-T6 aluminum alloys, Int. J. Adv. Manuf. Technol. 2016.

[20] M.A. Mofid, A.A. Zadeh, F.M. Ghaini, C.H. Gur, Submerged Friction Stir Welding (SFSW) Underwater and Under Liquid Nitrogen: An Improve Method to Join Al Alloys to Mg Alloys, Metallurgical And Materials Transactions **43**A (2012).

[21] X. Cao, M. Jahazi, Mater. Des. **30**, 2033-2042 (2009).

[22] S.M. Chowdhury, D.L. Chen, S.D. Bhole, X. Cao, Tensile properties of friction stir welded magnesium alloy: Effect of pin tool thread orientation and weld pith, Materials Science and Engineering A **527**, 606-607 (2010).

[23] S.H.C. Park, Y.S. Sato, H. Kokawa, Scr. Mater. **49**, 161-166 (2003).

[24] L. Huetsch, K. Herzberg, J. dos Santos , N. Huber, A study on local thermal and strain phenomena of high-speed friction stir-processed Mg AZ31, Weld World **57**, 515-521 (2013).

[25] S.H. Chowdhury, D.L. Chen, S.D. Bhole, X. Cao, P. Wanjara, Friction Stir Welded AZ31 Magnesium Alloys: Microstructure, Texture, and Tensile Properties, The Minerals, Matals & Materials Society and ASM International 2012.

[26] T. Balawender, R.E. Śliwa, T. Gałczyński, Zgrzewanie tarciowe z przemieszaniem blach ze stopu aluminium 2024, Hutnik, Wiadomości Hutnicze **8**, 7, 450-455 (2014).